PERIODICO di MINERALOGIA
established in 1930

DIPARTIMENTO
DI SCIENZE DELLA TERRA

SAPIENZA
UNIVERSITÀ DI ROMA

An International Journal of
Mineralogy, Crystallography, Geochemistry,
Ore Deposits, Petrology, Volcanology
and applied topics on Environment, Archaeometry and Cultural Heritage

Geochronology, geochemistry, and petrogenesis of the Dongshadegai K-feldspar granite in the northern margin of the North China Craton, China: Implications for Indosinian magmatism and related Au mineralization

Jianfei Fu [1,2,*], Sanshi Jia [1,3], Ende Wang [1,2], Yekai Men [1,3]

[1] Key Laboratory of Ministry of Education on Safe Mining of Deep Metal Mines, Northeastern University, Shenyang 110819, China
[2] School of Resource and Civil Engineering, Northeastern University, Shenyang 110819, China
[3] School of Resource and Materials, Northeastern University at Qinhuangdao, Qinhuangdao 066004, China

ARTICLE INFO

Submitted: April 2019
Accepted: August 2020
Available on line: October 2020

* Corresponding author:
fujianfei@mail.neu.edu.cn

DOI: 10.13133/2239-1002/17147

How to cite this article:
Fu J. et al. (2021)
Period. Mineral. 90, 85-101

ABSTRACT

As representative examples of alkaline magmatism and related mineralization in the northern margin of the North China Craton, the gold deposits within the Hadamengou Au-enriched region are dominated by K-feldspar-quartz vein-type gold mineralization. In contrast, the Dongshadegai pluton in the northern part of this region mainly consists of K-feldspar granite. In this study, we determined the U-Pb zircon age of the Dongshadegai pluton (236.0±2.7 Ma), indicating that this pluton was produced by middle Indosinian magmatism. The Dongshadegai pluton are characterized by high concentration of SiO_2 (70.4-72.5%), K_2O (K_2O/Na_2O=1.12-1.25) and total alkali (K_2O+Na_2O, 8.95-9.52%), and relatively low concentration of Al_2O_3 (13.83-14.8%). They are enriched in light rare earth elements (LREE/HREE, 18.04-21.65) and K, La, Ce, and Hf, and they are depleted in elements of Nb, Ta, P, Ti, and Sr, with weakly negative Eu anomalies (δEu=0.61-0.76). Thus, the overall lithogeochemistry of the Dongshadegai pluton resembles that of A-type granite, indicating that the pluton originated from an alkaline-enriched magma. According to the regional tectonic evolutionary history and the geochemical features of the pluton, we conclude that the Dongshadegai pluton formed in an extensional fault setting after a tectonic collision, and its corresponding age is consistent with the formation times of both the Hadamengou gold deposits and the Xishadegai Mo deposits. Based on a comprehensive analysis of the results of recent studies of regional tectonic magmatism and metallogenic processes, we suggest that a large-scale Au-Mo mineralization event occurred in the northern margin of the North China Craton resulted from Indosinian tectono-magmatic event. Compared with regional Late Mesozoic mineralization, the Indosinian mineralization play an important role in study area.

Keywords: Indosinian period; K-feldspar granite; zircon U-Pb; Au (Mo) mineralization; geochemistry.

INTRODUCTION

Within the Hadamengou Au-enriched region on the northern margin of the North China Craton (Figure 1), two large-scale gold deposits exist, Hadamengou and Liubagou; these deposits contain 100 t of proven Au resources with an average grade of 4.13 g/t (Hou et al., 2011; Zhang et al., 2012). These gold deposits are characterized by the development of K-feldspar-

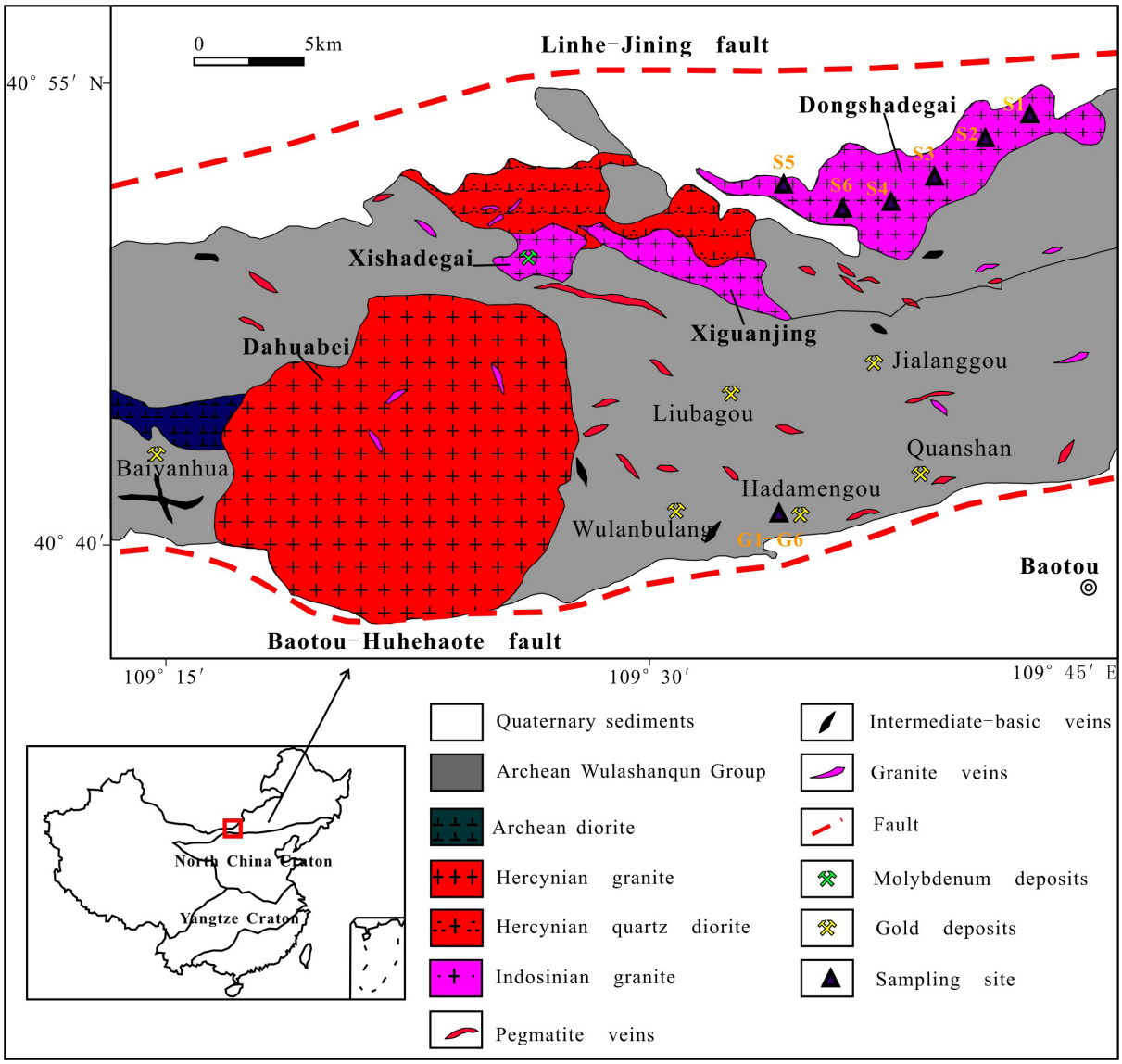

Figure 1. Geologic sketch map of the Hadamengou gold ore cluster at the northern margin of the North China Craton (modified after the Gold Headquarters of the CPAE, 1995).

quartz vein-type Au mineralization and are hosted in the amphibolite- to granulite- facies metamorphic rocks of the Archaean Wulashan Group. International scholars have paid much attention to these gold deposits since their discovery (Nie and Bjorlykke, 1994, 2005; Gan et al., 1994; Chen et al., 1996; Zhang et al., 1999; Miao et al., 2000; Hart et al., 2002). With continuous in-depth research and the increasing discovery of large quantities of both K-feldspar-quartz vein-type and K- and Si-altered rock type Au mineralization, it has become clear that K-feldspathization characterizes the Au mineralization in this region, which is also representative of the gold deposits located on the margins of the entire North China Craton. This result has consequently caused scholars to recognize the close relationship between K-enriched magmatism and Au mineralization in this region (Hou, 2011; Zhang, 2012). In turn, a key goal for gold deposit studies in this region is to define the evolution and formation period of the K-rich plutons, and this has become a focus of research since the discovery of the large Dongping gold deposit in the middle section of the K-rich plutons which are located on the northern margin of the North China Craton (Mao et al., 2011; Li et al., 2010; Chao et al., 2012).

There are four main plutons of varying scales in the Hadamengou Au-enriched region (Figure 1), namely, the Dahuabei pluton in the west and the Xishadegai,

Xiguanjing, and Dongshadegai plutons in the north. Occurrence of the Dahuabei pluton is complex, and veins are enriched in K-feldspar and widespread in the adjacent Wulanbulang gold deposit region. In turn, the contact zone of the Xishadegai pluton hosts medium-scale Mo deposits, and the pluton are characterized by K-alteration, which has been extensively studied. U-Pb dating indicated that the Dahuabei pluton formed during the Hercynian, whereas the Xishadegai pluton formed during the Indosinian (Miao et al., 2000, 2001; Zhang et al., 2011, Hou, 2010). However, studies on the Xiguanjing and Dongshadegai plutons are absent, and relationship between their petrogenesis and Au-Mo mineralization are remain controversial.

Recent prospecting and exploration activities have revealed the existence of medium-sized Jialanggou gold deposits in the southern region of the Dongshadegai pluton, and their mineralization is mainly characterized by the K-feldspar-quartz vein type and K- and Si-alteration rock type. The Jialanggou gold deposits and the Liubagou deposit in the north, together with the Wulanbulang-Hadamengou metallogenic belt in the south, form the Hadamengou Au-enriched region. It is currently believed that the metallogenic timing of the Jialanggou gold deposits largely ranged from the Hercynian to the Indosinian period (Nie et al., 2005; Zhao et al., 2009; Zhang et al., 2011; Hou, 2011; Gu et al., 2015) and that the Mo deposits in Xishadegai formed during the Indosinian period (Hou et al., 2010). In addition, relationship between petrogenesis and the formation of the Mo deposits and Au mineralization also is a hot topic in this region (Figure 2; Muller and Groves, 1997). In this study, we performed detailed zircon U-Pb dating on the Dongshadegai K-feldspar granite and characterized its whole-rock major and trace element contents and Pb isotopic composition. By comparing the Pb isotopic compositions of major gold deposits within this region and their metallogenic periods, our aims are to discuss the relationship between petrogenesis of the Dongshadegai pluton and the mineralization background. Furthermore, we use these data to discuss the implications for future prospecting work in other regions in the context of the entire northern margin of the North China Craton.

GEOLOGICAL SETTING AND PETROLOGY

The Dongshadegai pluton is located in the northern part of the Hadamengou Au-enriched region on the northern margin of the North China Craton. The exposed strata in this region primarily include the Archaean Wulashan Group and Quaternary alluvium. The Wulashan Group rocks dominantly comprise biotite-hornblende plagiogneiss, garnet-biotite plagiogneiss, hornblende-biotite plagioclase K-feldspar gneiss, hornblende mixed with a small amount of plagioclase, and leucoleptite. E-W-directed faults are present in this region; these faults mainly include the Baotou-Hohhot piedmont deep fault and the Linhe-Jining mountain rear deep fault, which control the spatial distribution of magma and metallogenic deposits. Multiple-period secondary magmatic intrusive rocks have developed in this region, their rock types consist of quartz-diorite, diabase, diabase porphyrite, granite, and granite-pegmatite. These rocks mainly compose the Dahuabei pluton in the western area of the Hadamengou Au-enriched region and the Xishadegai, Xiguanjing and Dongshadegai plutons in the north. In these intrusions, medium-sized Mo deposits exist in the Xishadegai pluton and its contact zone (Figure 1) (Hou et al., 2011).

The Dongshadegai pluton intrudes on the metamorphic rocks of the Wulashan group with a stock-like shape and is located close to the outcrop at the southern margin of the Linhe-Jining mountain rear deep fault. The pluton plane appears as an irregular downward-pointing triangle with an exposed area of approximately 25 km^2. From the margin to the centre of the pluton, banded facies are apparent; the marginal facies are fine- to medium-grained, and the internal facies exhibit medium- to coarse-grained textures. In addition, K-feldspar phenocrysts can be observed in some regions and show a porphyritic-like texture with varying particle sizes. These two types of textures show a progressively varying relationship. Previous petrologic studies have shown that the Dongshadegai pluton is dominantly composed of flesh-pink K-feldspar granite, followed by biotite K-feldspar granite. The K-feldspar granite shows a fine- to medium-grained hypautomorphic granular texture, and the dominant minerals are K-feldspar, plagioclase, quartz, and biotite; the biotite K-feldspar granite has a fine- to medium-grained hypautomorphic granular texture, and the dominant minerals are K-feldspar, plagioclase, quartz, and biotite (Figure 2), with a small amount of short columnar-like apatite (Gu et al., 2015).

SAMPLING AND ANALYTICAL METHODS

We collected samples for analysis from the Dongshadegai pluton (Figure 2) and the Hadamengou gold deposits. One plutonic rock was selected for combined cathodoluminescence (CL) imaging and zircon U-Pb age dating. Another 10 samples from pluton and gold deposits were chosen for Pb isotope analysis, and six samples from the Dongshadegai pluton were selected for analysis of their whole-rock major and trace element concentrations.

Whole-rock geochemistry

Analyses of the major, trace and rare earth elements were performed in these samples of the Dongshadegai pluton

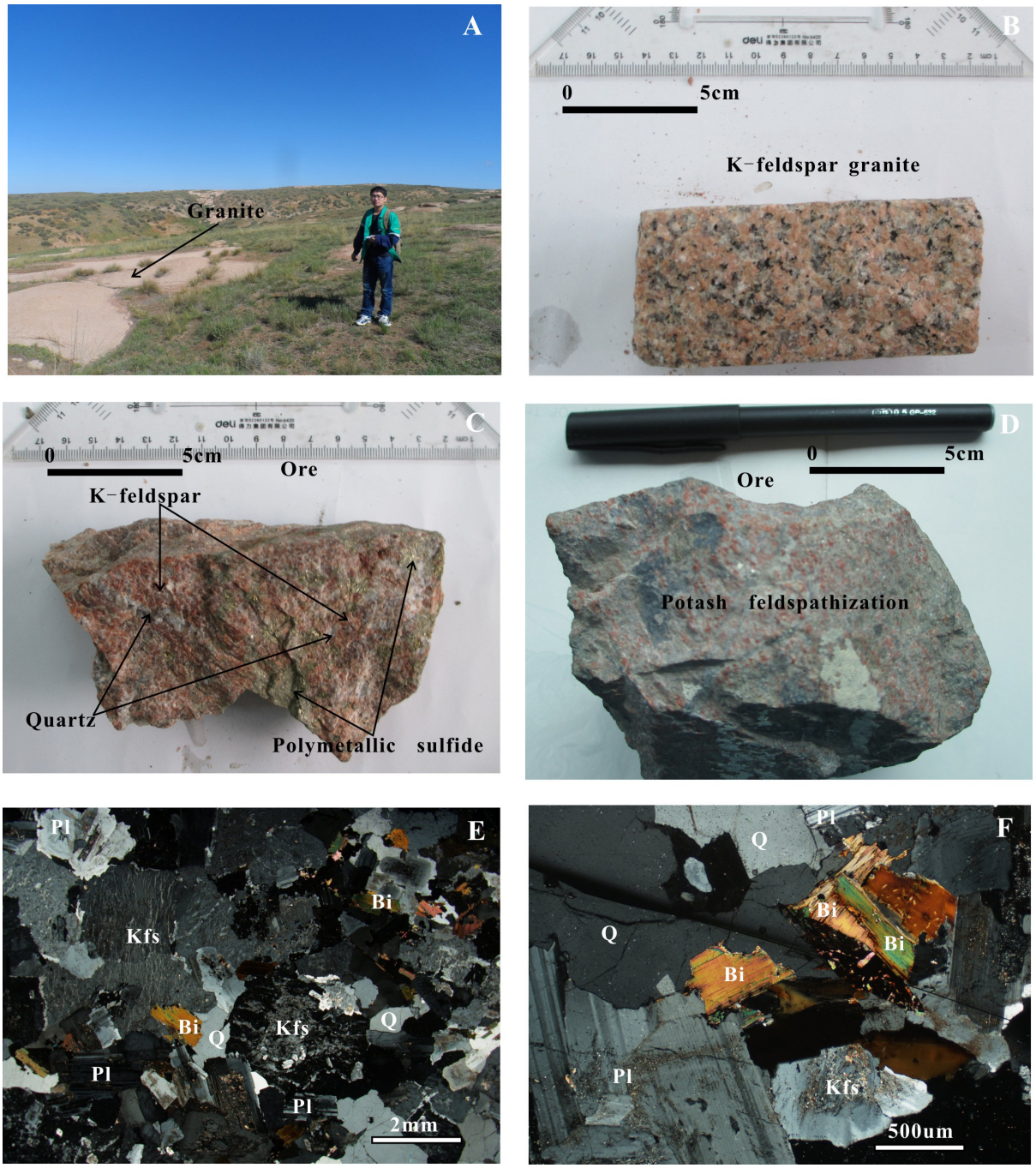

Figure 2. Field photos and photomicrographs of the Dongshadegai granite. A) Granitic pluton outcrop; B) K-feldspar granite; C) K-feldspar-quartz vein type gold ore; D) K-feldspar alteration type gold ore; E) K-feldspar granite; F) K-feldspar granite. Abbreviations: Bi, biotite; Kfs, K-feldspar; Pl, plagioclase; Q, quartz.

in the laboratory of ALS Minerals-ALS Chemex Co. Ltd (Table 1). First, weathering products were removed from the surface of each sample. Then, each sample was rinsed with Millipore-purified water and was air dried. Subsequently, each sample was broken into fragments with diameters ranging from 1 to 2 cm. The fragments were then placed in a vibrating mill and ground into 200-mesh powder. After each sample was ground, the sample chamber of the vibrating mill was rinsed with Millipore-purified water to prevent cross-contamination between

Table 1. Major element composition (wt%) and trace and rare earth element compositions (ppm) of the Dongshadegai K-feldspar granite.

Sample No.	S1	S2	S3	S4	S5	S6
Lithology	K-feldspar granite					
Major elements (%)						
SiO_2	72.50	70.40	72.21	72.44	70.70	71.21
TiO_2	0.28	0.33	0.29	0.32	0.36	0.33
Al_2O_3	14.30	14.80	13.88	13.83	14.64	14.68
Fe_2O_3	1.01	0.99	0.87	1.08	1.12	1.10
FeO	0.86	1.19	0.94	0.93	1.11	0.95
MnO	0.04	0.05	0.05	0.04	0.05	0.04
MgO	0.41	0.46	0.40	0.43	0.47	0.45
CaO	1.14	1.24	1.19	1.12	1.26	1.22
Na_2O	4.10	4.40	4.12	4.17	4.46	4.42
K_2O	5.11	5.07	4.86	4.78	5.01	5.10
P_2O_5	0.08	0.09	0.08	0.08	0.09	0.09
BaO	0.11	0.11	0.10	0.09	0.11	0.12
Cr_2O_3	0.02	0.01	0.01	0.01	<0.01	0.01
SrO	0.03	0.03	0.03	0.03	0.04	0.04
LOI	0.32	0.30	0.49	0.37	0.44	0.58
Total	100.41	99.60	99.62	99.82	99.98	100.45
A/CNK	0.997	0.988	0.977	0.983	0.973	0.978
A/NK	1.165	1.163	1.153	1.149	1.147	1.148
Rare earth elements (ppm)						
La	49.9	52	50.1	53.6	56.4	55.2
Ce	88.5	102.5	85.3	98.3	113.5	103.5
Pr	9.15	11.00	8.20	9.57	11.40	10.20
Nd	26.3	32.6	24.6	29.5	36.9	32.3
Sm	3.84	4.84	3.60	4.41	5.35	4.77
Eu	0.76	0.90	0.80	0.84	0.97	0.87
Gd	2.64	3.36	2.60	3.17	3.96	3.30
Tb	0.38	0.48	0.30	0.41	0.53	0.45
Dy	2.05	2.61	1.90	2.48	3.09	2.68
Ho	0.40	0.51	0.40	0.48	0.61	0.55
Er	1.17	1.46	1.20	1.47	1.73	1.21
Tm	0.18	0.23	0.30	0.25	0.30	0.26
Yb	1.22	1.43	1.30	1.64	1.94	1.67
Lu	0.20	0.23	0.20	0.25	0.28	0.24
Y	12.1	15.4	11.5	14.7	18.7	16.1
ΣREE	186.69	214.15	180.8	206.37	236.96	217.2
LREE	178.45	203.84	172.60	196.22	224.52	206.84
HREE	8.24	10.31	8.20	10.15	12.44	10.36
LREE/HREE	21.65	19.77	21.04	19.33	18.04	19.96
LaN/YbN	29.34	26.08	27.64	23.44	20.85	23.71
δEu	0.69	0.64	0.76	0.65	0.61	0.63
δCe	0.94	1.00	0.94	0.98	1.04	0.99

Table 1. ... Continued

Sample No.	S1	S2	S3	S4	S5	S6
Lithology			K-feldspar granite			
Major elements (%)						
Trace elements (ppm)						
Ga	18.70	19.20	18.15	18.50	18.75	19.00
Rb	113.00	100.00	123.00	117.00	106.50	111.00
Ba	970.00	990.00	850.00	902.00	952.00	1055.00
Th	16.60	13.70	16.00	16.45	12.15	12.45
U	2.30	3.80	3.00	2.32	3.77	2.09
K	43000.00	43100.00	38500.00	39100.00	41000.00	40200.00
Ta	1.79	1.92	1.59	2.20	2.30	2.30
Nb	25.10	27.80	21.60	27.70	29.80	29.20
Sr	276.00	306.00	234.00	280.00	302.00	312.00
P	330.00	380.00	360.00	390.00	440.00	410.00
Zr	41.20	34.00	47.50	244.00	328.00	234.00
Hf	1.70	1.50	1.90	6.90	8.80	6.80
Ti	1670.00	2040.00	1580.00	1910.00	2190.00	1910.00

samples. Major element analyses were performed with an Axios X-ray fluorescence spectrophotometer using the lithium metaborate glass melting method. The analytical accuracy was greater than 5%. Trace and rare earth element analyses were performed with an Elan 9000 ICP-MS instrument using the high-temperature high-pressure, four-acid digestion method and the lithium borate melting method, respectively. The analytical accuracy was greater than 5%.

Zircon U-Pb dating

The zircon grains used for U-Pb dating by laser ablation inductively coupled plasma mass spectrometry (LA-ICP-MS) were separated from the S4 sample of the Dongshadegai pluton using conventional heavy liquid and magnetic separation methods. Representative zircon grains were hand-picked under a binocular microscope, mounted on an epoxy resin disk, and polished down to nearly half the section width to expose their internal structures for LA-ICP-MS analysis. Zircons were documented with transmitted and reflected light photomicrographs as well as with CL imaging to reveal their internal structures (Figure 3), and the mount was vacuum-coated with high-purity gold. Zircon U-Pb dating analysis was conducted with an LA-ICP-MS at the ALS Chemex (Guangzhou, China) Co., Ltd. (Table 2). The analytical procedures used here were described by Jackson et al. (2004). Common Pb correction was performed following the method proposed by Anderson (2002). The analyses presented here have been corrected assuming recent Pb loss. Data processing was carried out using the Isoplot programmes of Ludwig (2001).

Pb isotope analysis

The Pb isotope compositions of the Dongshadegai pluton and the gold ore of the Hadamengou gold deposits were determined using high-resolution sector field inductively coupled plasma mass spectrometry (HR-ICP-SFMS) at the ALS Chemex Co., Ltd (Table 3).

The sample was combined with nitric acid, hydrochloric acid and hydrofluoric acid for microwave digestion, and the compositions of Pb isotopes were determined using HR-ICP-SFMS. If the Pb content was low, separation was required, and the digested solution was evaporated to dryness. In this case, 3 mol of nitric acid was added, and Pb was separated using an Eichrom ion exchange resin. The Pb in the sample solution to be tested was adjusted to an appropriate concentration, and the internal standard (Tl) was added so that the mass fractionation of Pb would be corrected.

The Pb isotopes were determined using HR-ICP-SFMS and the data were normalized using an internal standard (Tl isotope ratio) and external calibration (natural Pb material standard). Each digested sample was tested twice to obtain its standard deviation SD (test results were reported together). If the Pb content in the sample was sufficient, the relative deviation (RSD) was generally less than 0.1-0.2%. The allowable RSD of the laboratory control was <0.2%.

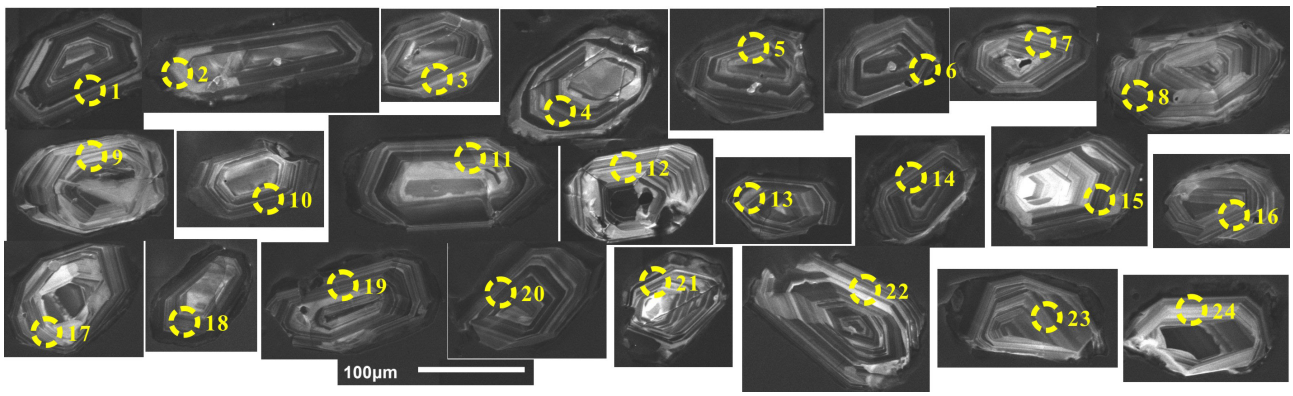

Figure 3. CL images of zircons in the K-feldspar granite from the Dongshadegai pluton.

Table 2. LA-ICP-MS U-Pb analyses of zircons of the K-feldspar granite from Dongshadegai.

Spot	Ratio of isotope						Apparent age/Ma					
	$^{207}Pb/^{206}Pb$	1σ	$^{207}Pb/^{235}U$	1σ	$^{206}Pb/^{238}U$	1σ	$^{207}Pb/^{206}Pb$	1σ	$^{207}Pb/^{235}U$	1σ	$^{206}Pb/^{238}U$	1σ
1	0.0515	0.0030	0.2666	0.0182	0.0365	0.0008	261	11	240	15	231	5
2	0.0521	0.0053	0.2728	0.0176	0.0382	0.0009	292	19	245	14	242	5
3	0.0518	0.0029	0.2714	0.0180	0.0390	0.0007	276	25	244	14	247	4
4	0.0537	0.004	0.2783	0.0198	0.0380	0.0007	358	13	249	16	240	4
5	0.0537	0.0038	0.2781	0.0200	0.0363	0.0008	357	16	249	16	230	5
6	0.0563	0.0035	0.2732	0.0230	0.0349	0.0007	463	14	245	18	221	4
7	0.0523	0.0053	0.2677	0.0150	0.0390	0.0010	297	19	241	13	247	7
8	0.0550	0.0035	0.2815	0.0300	0.0367	0.0009	410	26	252	14	233	5
9	0.5070	0.0027	0.2603	0.0210	0.0360	0.0008	229	12	235	17	228	5
10	0.0550	0.0043	0.2861	0.0160	0.0370	0.0007	413	35	255	12	234	4
11	0.0512	0.0034	0.277	0.0190	0.0383	0.0090	248	26	248	15	242	6
12	0.0596	0.0035	0.2977	0.0250	0.0360	0.010	589	13	265	19	228	5
13	0.0543	0.0050	0.2932	0.0175	0.0388	0.0008	382	14	261	15	245	5
14	0.0571	0.0062	0.2925	0.0290	0.0370	0.0007	496	31	260	22	234	4
15	0.0550	0.0041	0.2755	0.0200	0.0359	0.0006	412	21	247	16	227	4
16	0.0498	0.0036	0.2621	0.0190	0.0371	0.0009	184	21	236	14	235	5
17	0.0510	0.0041	0.2690	0.0260	0.0370	0.0008	241	12	242	21	234	5
18	0.0566	0.0032	0.2759	0.0142	0.0365	0.0009	435	19	247	11	231	6
19	0.0511	0.0031	0.2654	0.0172	0.0368	0.0010	245	12	239	15	233	7
20	0.0542	0.0041	0.2865	0.0186	0.0382	0.0009	378	20	256	15	242	6
21	0.0536	0.0033	0.2868	0.0160	0.0374	0.0010	353	17	256	12	237	6
22	0.0539	0.004	0.2793	0.0192	0.0373	0.0007	368	20	250	15	236	4
23	0.0542	0.0042	0.2810	0.0210	0.0390	0.0011	380	16	251	16	247	8
24	0.0507	0.0027	0.2626	0.0193	0.0376	0.0009	226	13	237	15	238	5

Table 3. Pb isotope composition of the Dongshadegai K-feldspar granite and gold deposits in the research area.

Sample No.	Description	$^{206}Pb/^{204}Pb$	$^{208}Pb/^{204}Pb$	$^{207}Pb/^{204}Pb$	Data sources
S1	K-feldspar granite	19.340	39.695	15.617	This study
S2		18.426	39.085	15.614	
S3		18.386	39.180	15.600	
S4		19.326	39.538	15.610	
G1	Gold ore	17.451	37.467	15.424	This Study
G2		17.494	37.520	15.443	
G3		17.312	37.413	15.407	
G4		17.334	37.414	15.414	
G5		17.281	37.394	15.411	
G6		17.375	37.436	15.423	
h1	K-feldspar granite	17.113	37.200	15.377	Hou et al.,2011
h2		17.323	37.051	15.387	
h3		16.838	36.910	15.358	
h4		17.156	37.169	15.397	

RESULTS

Whole-rock geochemistry

The whole-rock major and trace element data of the six samples from the Dongshadegai K-feldspar granite, are presented in Table 1 and Figure 4.

Figure 4 shows the major element compositions of these samples (Figure 4A and 4B), in which their SiO_2 contents range from 70.4% to 72.5% and their K_2O+Na_2O contents range from 8.95% to 9.52%; thus, the Dongshadegai K-feldspar granite samples are characterized by Si and alkaline enrichment and relative K enrichment. The aluminous saturation index (A/CNK) values of the Dongshadegai K-feldspar granite samples range from 0.973 to 0.997, indicating that the pluton is a weakly peraluminous granite (Figure 4C). These A/CNK values are close to those of A-type (1.04) and standard (1.05) granites and lower than that of S-type granite (1.18); the samples from this pluton also plot within the range of A-type granites on the K_2O-Na_2O plot (Figure 4D). Thus, overall, the Dongshadegai pluton resembles an A-type granite as it is characterized by alkaline enrichment.

The rare earth element (REE) contents of the six samples are relatively high, with ΣREE values ranging from 180.8 ppm to 236.96 ppm. When plotting the REE distribution patterns normalized to those of chondritic meteorites (Figure 5A), the samples generally show REE patterns enriched in LREE, with LREE/HREE ratios ranging from 18.04 to 21.65 and high $(La/Yb)_N$ values (20.85-29.34). In addition, the samples also have moderate negative Eu anomalies (0.61-0.76).

On the trace element spidergrams (Figure 5B), the Dongshadegai K-feldspar granite samples show consistent trace element distributions that are characterized by depletion of Nb, Ta, P, Ti, and Sr and enrichments of K, La, Ce, and Hf. Specifically, Ti depletion indicates the involvement of crustal material in the magma, as the refractory element Ti rarely moves to the melt and is mainly present in the remaining source region, whereas K and La are usually enriched in the melt and may reflect a crustal origin (Miao et al., 2003; Brown et al., 1984; Hou et al., 2011).

Zircon U-Pb chronology

CL images of representative zircon grains are shown in Figure 3. These zircons are generally euhedral, short to long prismatic, colourless, and transparent. The crystal length ranges from 100 to 200 mm, and the length-to-width ratios ranges from 1:1 to 4:1. Most of the zircons show oscillatory or planar zoning in CL images (Figure 3), similar to those typically observed in igneous rocks.

Twenty-four zircons from the Dongshadegai granite were analysed (Table 2). The results are plotted on a Concordia diagram in Figure 6. Twenty-three analyses yielded concordant ages and provided a weighted mean age of 236.0±2.7 Ma (MSWD=1.6).

Pb isotopes

A total of 10 samples were performed Pb isotopic analysis, including four K-feldspar granite samples collected from the Dongshadegai pluton and six gold ore samples collected from the Hadamengou gold deposits (Table 3). Their Pb isotopic compositions are as follows:

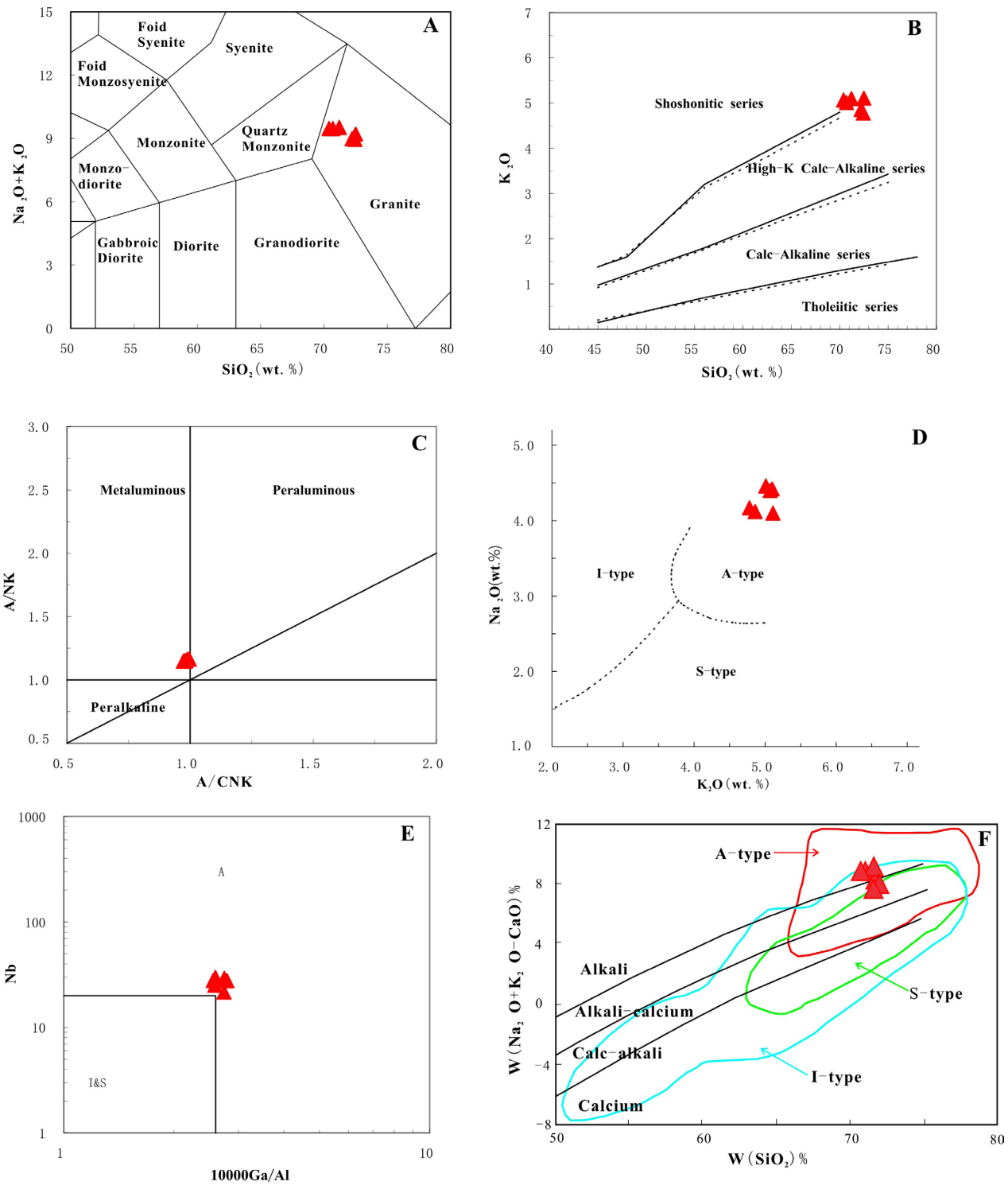

Figure 4. (A) TAS diagram (modified after Middlemost, 1994); (B) SiO_2 vs K_2O (modified after Rickwood, 1989); (C) A/NK vs A/CNK (modified after Maniar and Piccolo, 1989); (D) K_2O vs Na_2O (modified after Collins et al., 1982); (E) Nb vs 10000Ga/Al (modified after Whalen et al., 1987); (F) (Na_2O+K_2O-CaO) vs SiO_2 (modified after Frost et al., 2001).

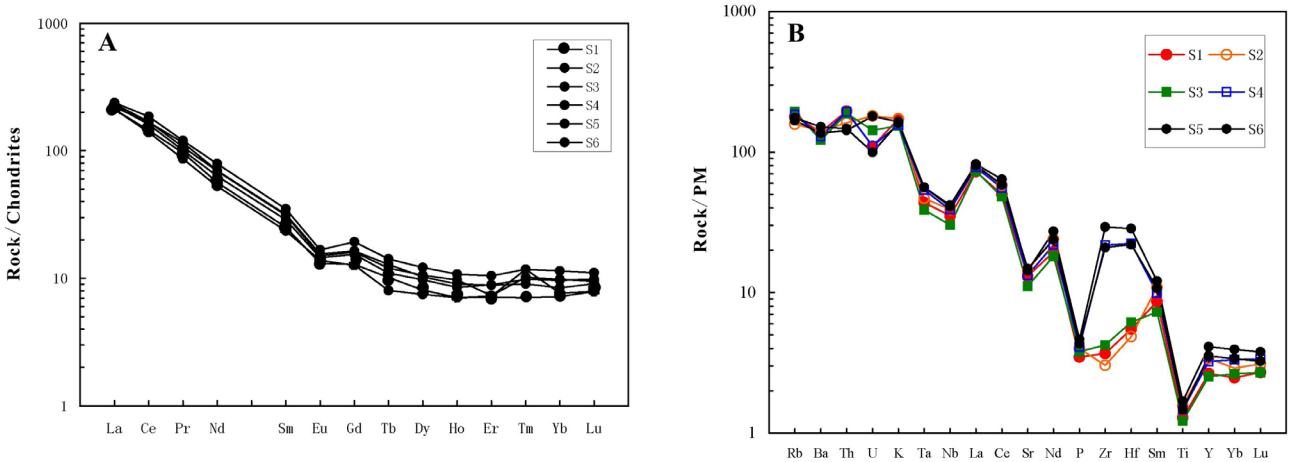

Figure 5. Normalized REE and trace element patterns for the Dongshadegai K-feldspar granite. Chondrite and primitive mantle data were obtained Boynton (Boynton, 1984) and Sun & McDonough (Sun and McDonough ,1989).

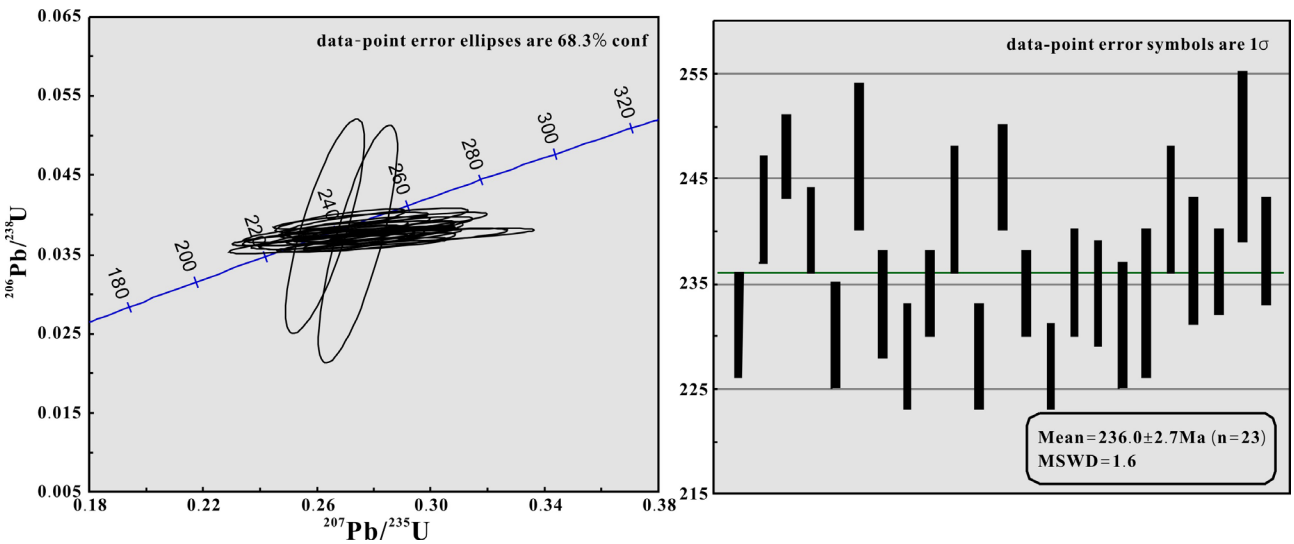

Figure 6. Zircon U-Pb Concordia diagrams of K-feldspar granite from Dongshadegai in North China.

(1) Four K-feldspar granites yield $^{206}Pb/^{204}Pb$ ratios of 18.386-19.340, $^{207}Pb/^{204}Pb$ ratios of 15.600-15.617 and $^{208}Pb/^{204}Pb$ ratios of 39.085-39.695; (2) Six gold ore samples yield $^{206}Pb/^{204}Pb$ ratios of 17.281-17.494, $^{207}Pb/^{204}Pb$ ratios of 15.407-15.443 and $^{208}Pb/^{204}Pb$ ratios of 37.394-37.520. We plotted the results of the Pb isotopes in Figure 7 for comparison. The Pb isotopic composition of gold ore in this study and granitic pluton (data published by Hou et al., 2011) are similar, and they plotted on the area between mantle and lower crust, further suggesting that the Pb composition were derived from mixed crustal and mantle sources (Figure 7A). While the Pb compositions of K-feldspar granites straddle orogene and upper crust (Figure7A), their distribution are characterized by linear correlation related to gold ore and granitic plutons (Figure7A and B). The result suggests these K-feldspar granites are related to mineralization, and the difference of Pb isotope could result from metamorphism.

DISCUSSION

Age of the Dongshadegai K-feldspar granite

Previously, Miao et al. (2001) determined the formation age of the Dahuabei pluton (i.e., the largest-scale pluton in this region) to be 353±7 Ma based on SHRIMP U-Pb dating of zircons; later, Li et al. (2009) reduced the U-Pb age of these zircons to 330±10 Ma using LA-ICP-MS

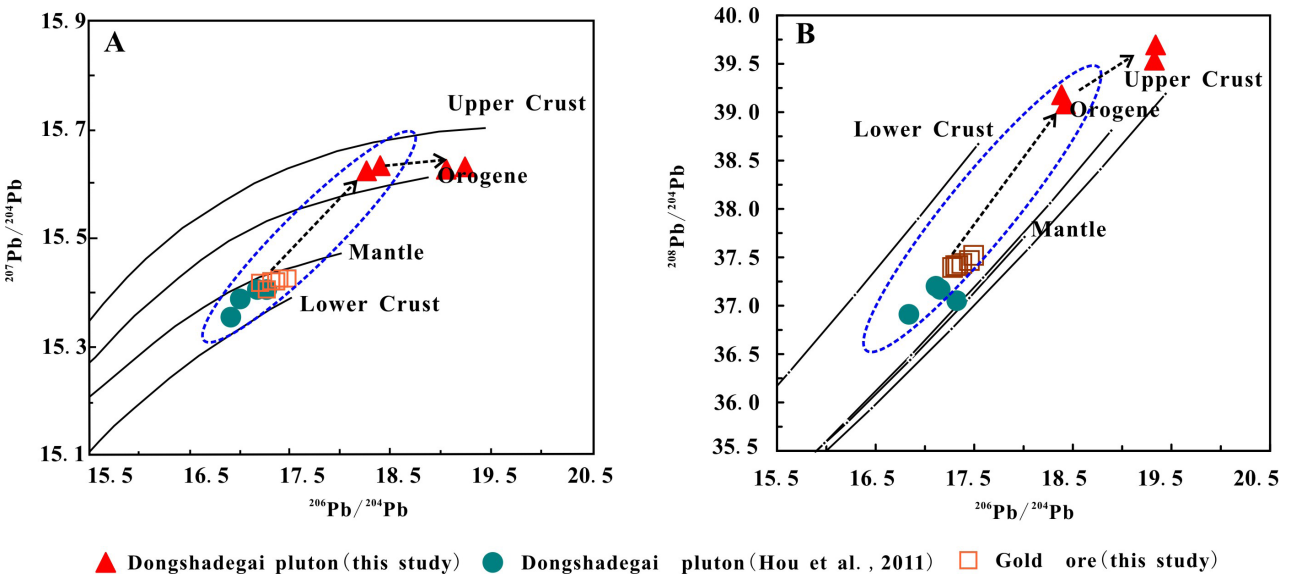

Figure 7. (A) Plots of $^{207}Pb/^{204}Pb$ vs $^{206}Pb/^{204}Pb$ and (B) $208Pb/^{204}Pb$ vs $^{206}Pb/^{204}Pb$ showing the relationships between the Pb isotope compositions of in the research area and the evolution curves of the upper crust, lower crust, orogene and mantle, respectively (modified after Zartman and Doe, 1981).

dating. Additionally, Nie and Bjorlykke (1994) inferred the formation age of the Dahuabei pluton to be 322±22 Ma based on Rb-Sr isochron analysis. Thus, previous studies have consistently concluded that the Dahuabei pluton formed during the early to middle Hercynian period. Hou et al. (2011) determined the age of the Xishadegai pluton, which hosts medium-sized Mo deposits, to be 222.9±0.82 Ma using LA-ICP-MS U-Pb dating on zircon, whereas Re-Os isochron analysis of molybdenite yielded an age of 226.4±3.3 Ma. Because the Xiguanjing pluton is largely exposed at the surface and thus suffers from severe weathering, little dating has been performed in this region.

Zhao et al. (2009) and Hou et al. (2011) previously dated the Dongshadegai pluton and obtained U-Pb zircon ages of 198.5 Ma and 221.1±2.1 Ma. We also conducted a U-Pb isotopic analysis of zircons separated from the Dongshadegai K-feldspar granite in the Hadamengou Au-enriched region using LA-ICP-MS and obtained a weighted mean age of 236.0±2.7 Ma, which represents the formation age of the Dongshadegai pluton; this age is consistent with that of the Xishadegai pluton and the formation age of the Mo deposits within the Xishadegai pluton, which were all formed in the Indosinian period.

The results of the studies discussed above demonstrate that at least two periods of magmatism have occurred in the Hadamengou Au-enriched region. The first is the Hercynian tectono-magmatic event, which is represented by the Dahuabei pluton, and the second is the Indosinian magmatism, which is represented by the Xishadegai and Dongshadegai plutons. Recently, Zhang et al. (2018) performed zircon LA-ICP-MS U-Pb dating on the Xishadegai pluton, which yielded a weighted mean age of 235.1±2.0 Ma. These dating results showed that there are at least two ages of formation of the Xishadegai and Dongshadegai plutons, 222.9±0.82 Ma and 235.1±2.0 Ma, 221.1±2.1 Ma and 236.0±2.7. The above results indicate that multiple periods of magmatic intrusion may have occurred during the Indosinian period in the Xishadegai and Dongshadegai plutons in the research area.

It is worth mentioning that Indosinian magmatism occurred in areas other than the studied area. At the northern margin of the North China Craton, the whole-rock Rb-Sr isotope age of syenite from the Fanshan pluton, Zhulu, Hebei, was determined to be 218 Ma (Mou and Yan, 1992); the whole-rock Rb-Sr isotope age of alkaline granite from the Guangtoushan pluton, Pingquan, Hebei, was 194 Ma (Han et al., 1993); the U-Pb age of zircons from the Dushan pluton in Jidong was 223±2 Ma (Luo et al., 2003); and the U-Pb age of porphyritic zircons from the Jiguanshan pluton, Chifeng, Inner Mongolia, was 245±2.7 Ma (Zeng et al., 2009). In Fengcheng, Liaoning, on the eastern margin of the North China Craton, the Rb-Sr isotope age of the Bolinchuan syenite was determined to be 218 Ma, and the age of the Saima syenite was 244 Ma (Zhou et al., 1996); additionally, the U-Pb age of zircons from the Jiapigou Au-deposit granite vein was 223±2 Ma (Luo et al., 2002). Together, these results indicate that alkaline-rich magmatism apparently

occurred during the Indosinian period on the northern margin of the North China Craton, which was the product of Indosinian magmatism.

Petrogenesis of the Dongshadegai granite

The geochemical characteristics of the Dongshadegai pluton indicate that it is A-type granite (Figure 4D, 4E and 4F). Moreover, the Dongshadegai K-feldspar granite samples have high alkaline content, relative K enrichment, and A/CNK values of 0.971-0.997 (Table 1). Thus, we conclude that the Dongshadegai K-feldspar granite is a weakly peraluminous A-type granite with K and alkaline enrichment.

The following three genetic models have been proposed for the genesis of A-type granites: (1) the differentiation of alkaline basalts from mantle sources (Frost and Frost, 1997; Mushkin et al., 2003); (2) the partial melting of F-Cl-rich lower crust after the extraction of I- or S-type granitic magma residue in granulite (Collins et al., 1982; Whalen et al., 1987; King et al., 2001); and (3) the mixing of crust and mantle material (Mingram et al., 2000; Yang et al., 2006) and partial melting of crustal rocks (Collins et al., 1982; Creaser et al., 1991; Skjerlie and Johnston, 1992; Martin, 2006; Gao et al., 2016; Honarmand et al., 2017).

The lack of contemporary basalts in the research area indicates that the amount of granitic melt produced by the differentiation of alkaline basalts is too small to have formed the voluminous granitoids. These granites are all enriched in large ion lithophile elements and relatively depleted of high field strength elements (Nb and Ta), and they are also strongly depleted of Sr, P, Eu and Ti. These characteristics indicate that the primary magma of the A-type granite was mainly generated by the partial melting of crustal material. However, the high Nb/Ta ratios of these A-type granites fall between those of the primary mantle and mature crustal rocks, indicating that the A-type granites could have been derived from the partial melting of the delaminated lower crust with minor mantle contribution.

Additionally, the Pb isotope data of the Dongshadegai pluton indicate that this material originated from between the mantle and the lower crust (Figure 7), representing a mixed crust and mantle source, which implies that the granite in the study area is a K-feldspar-rich contaminated granite. The K-feldspar-rich contaminated granite was generated during the relaxation period after a collision event due to the *in situ* intrusion of mantle-derived magma into the crust (Figure 8), reflecting the transition from compression to extension, whereas K-feldspar-poor contaminated granite was found in the crust and formed on top of the thin subduction zone (Zhan, 1998). All of these data indicate that the A-type granites may be formed by the mixing of mantle-derived magmatic intrusions and crust-derived magmatism in an extensional tectonic setting (Figure 9).

Geodynamic implications

Petrogenetically, the Dongshadegai K-feldspar granite is an A-type granite. More specifically, on the plot of Yb/Ta vs. Y/Nb defined by Eby (1992), this rock plots within the A1 subseries, indicating that it formed in a similar tectonic environment as oceanic-island basalt (OIB), i.e., in an extensional setting. However, on the plots of Rb-Yb+Nb, Al_2O_3-SiO_2, and R2-R1, these samples plot in the field of granite that formed after collisions or post-orogenic granite, indicating that the Dongshadegai pluton likely formed after a collisional event in an extensional tectonic environment (Figure 8).

The regional tectonic evolutionary history of this area can be defined as follows. Prior to the Paleozoic, the research area was located within the Paleo-Asian ocean and was connected to the North China plate in the south and the Siberian plate in the north (Windley et al., 2007; Zhao et al., 2010). Since the Late Paleozoic, the Paleo-Asian ocean has subducted under the North China plate and the Siberian plate from its southern and northern sides, respectively, and the northern margin of the North China plate evolved into a continental margin characterized by Andean-type activity, where large areas of intermediate-felsic volcanic rocks and granite developed (Lamb and Badarch, 1997; Badarch et al., 2002). Recent studies of tectonic systematics, strata sequences, palaeobiology and petrology have shown that the final collision and convergence of the North China plate and the Siberian plate occurred during the Late Permian to Early Triassic period. After collision at 250 Ma, the northern margin of the North China Craton entered a post-collision tectonic magmatic evolutionary stage (Chen, 2000; Wu et al., 2002, 2004; Xiao et al., 2003; Li, 2006; Wu et al., 2007; Windley et al., 2007; Xiao et al., 2009). Due to crustal gravitational collapse, lithospheric delamination, and asthenospheric upwelling, the research area transitioned to an apotectonic extensional environment as a result of the formation of a series of alkaline granite intrusions (Wu et al., 2002, 2004; Nie et al., 2011). Concomitantly, Au and Mo polymetallic deposits formed, largely due to the occurrence of magmatism, e.g., the Jiguanshan Mo deposit, Jiapigouerdaogou gold deposit, Yuanbaoshan Mo deposit, and Dasuji Mo deposit on the northern margin of the North China Craton (Zeng et al., 2009; Wan et al., 2009; Liu et al., 2010).

Magmatism and Au-polymetallic mineralization

Because of the Indosinian alkaline magmatism that occurred in this region, medium-sized Mo deposits developed in the Xishadegai pluton and its contact zone,

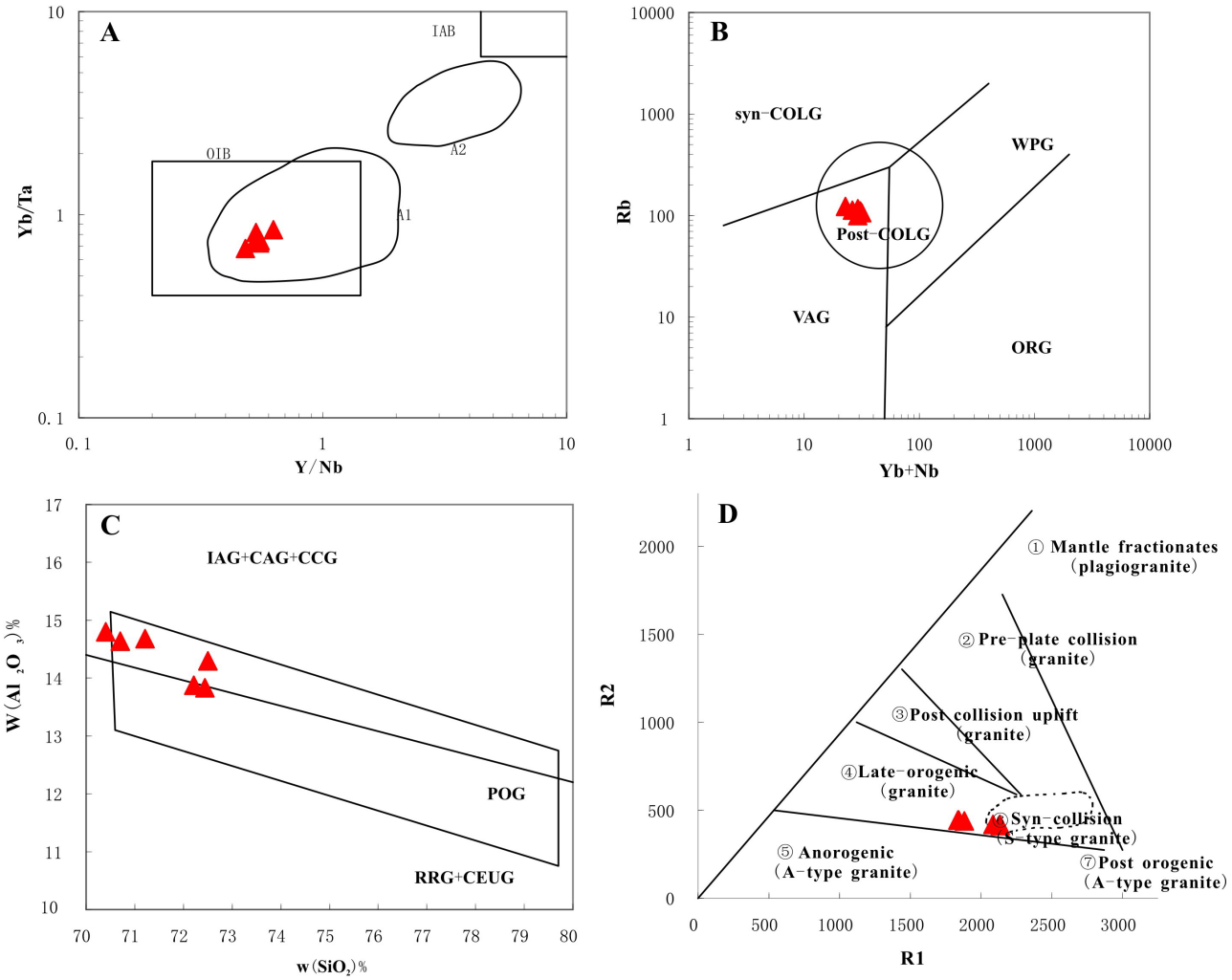

Figure 8. Tectonic discrimination diagrams for the Dongshadegai K-feldspar granite. (A) Yb/Ta vs Y/Nb diagram (modified after Eby, 1992); (B) Rb vs Yb+Nb diagram (modified after Pearce, 1996); (C) Al_2O_3 vs SiO_2 diagram (modified after Maniar and Piccoli, 1989); (D) R2 vs R1 diagram (modified after Batchelor et al., 1985).
Abbreviations: OIB, oceanic-island basalts; IAB, island-arc basalts; A1 and A2, various A-type granitoid suites; syn-COLG, syn-collision granites; WPG, within-plate granites; Post-COLG, post-collision granites; VAG, volcanic arc granites; ORG, ocean ridge granites. IAG, island-arc granites; CAG, continental arc granites; CCG, continental collision granites; POG, post-orogenic granites; RRG, rift related granites; CEUG, continental collision uplift related granites.

and Au and Mo mineralization has been found in the deep regions of the Hadamengou and Liubagou gold deposits. Extensive Au mineralization of the K-feldspar-quartz vein type and the K- and Si-altered rock type developed in the research area. Because the Dongshadegai pluton comprises K-feldspar granite, it is necessary to discuss the relationship between pluton formation and the Au and Mo mineralization in this region. On the isotopic composition plot (Table 3 and Figure 7). The Pb isotopic compositions of the Dongshadegai pluton and Hadamengou gold deposits indicate that the ore forming fluids and ore metal were derived from similar sources (Figure 7A; Zartman and Doe, 1981; Hou et al., 2011). Taking account of the petrogenesis of the K-feldspar granite, we suggest that the ore metals were mainly derived from lower continental crust with minor contribution of mantle. The linear distribution of Pb isotope straddle lower crust and orogene, suggesting that the study area was subjected later orogeny, and resulted in the differentiation of Pb isotope composition (Figure 7B). The geochronological data of the granitic plutons also indicate that the tectono-magmatism last for 15 Ma, which is consistent with the differentiation of Pb isotopic composition of granitic plutons. The formation of the Hadamengou deposits was

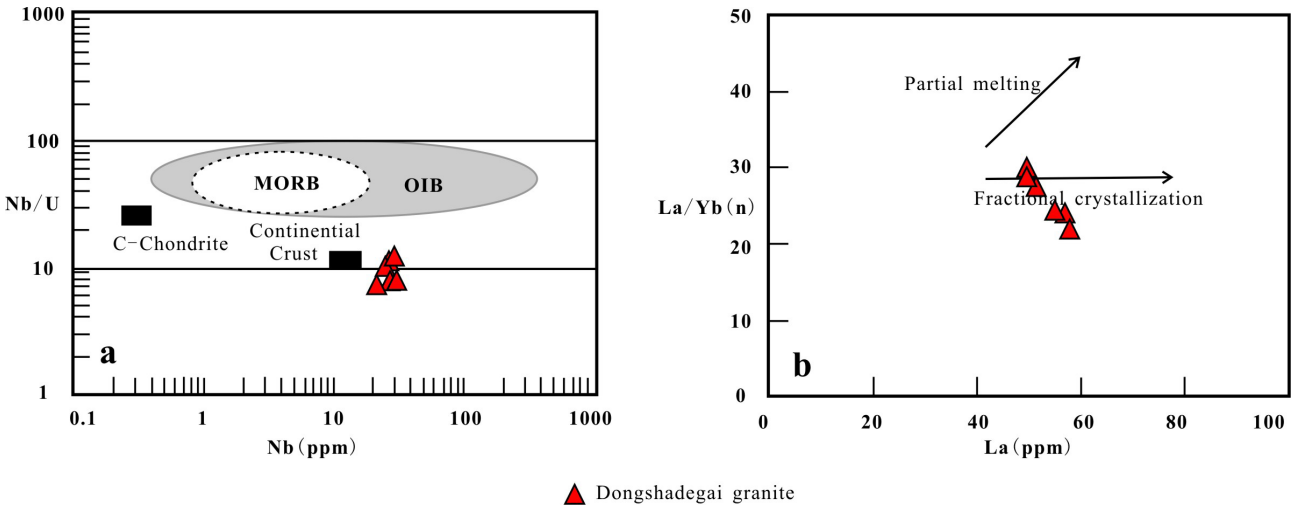

Figure 9. a) Nb/U vs Nb, b) La(n)/Yb(n) vs La for Dongshadegai granite (Moghadam et al., 2015). Abbreviations: MORB, mid-ocean ridge basalt; OIB, oceanic-island basalt.

caused by Indosinian metallogenic processes that occurred at 240±3 Ma (Nie et al., 2005), which is close to the age of the Dongshadegai pluton. Thus, the Dongshadegai pluton and the Hadamengou gold deposits were both produced by tectonic magmatism during the same period.

The relationship between the Dongshadegai pluton and the gold deposits in this region illustrates that during the Triassic period, with the end of the collisional and connecting activities between the North China plate and the Siberian plate, the tectonic units along the convergence belt became relaxed, and this change resulted in large-scale continental chasmic activities that provided favourable conditions for alkaline-rich magmatism and the upwelling of Au-containing fluids. In terms of the geologic characteristics of the region, a series of intrusive rocks of varying scales formed at the northern margin of the North China Craton during the Indosinian period; Au and Mo polymetallogenic deposits of different scales were produced in the internal and external contact belts of the pluton and its surrounding strata (Mao and li, 2001; Zeng et al., 2009; Wan et al., 2009; Liu et al., 2010; Song et al., 2011; Cai et al., 2011); additionally, the characteristic Au mineralization of the K-feldspar-quartz vein type and K- and Si-altered rock type also occurred in this region. Globally speaking, alkaline-rich magmatism is also closely related to Au mineralization (Muller et al., 1997; Jensen and Barton, 2000; Sillitoe, 2002); typical examples include the Cripple Creek gold deposit in the U.S. (Kelley and Ludington, 2002), the Kirkland Lake gold deposits in Canada (Kerrich and Watson, 1984), and the large-scale Emperor gold deposits in Matanitu (Ahmad and Walshe, 1990).

The above studies have shown that after the collision and merger of the North China and Siberian plates during the Hercynian period, the research area entered a post-collisional extensional environment during the Indosinian period, which resulted in a series of tectonic-magmatic events on the northern margin of the North China Craton. In particular, alkaline-rich magmatism produced an especially significant amount of Au polymetallic deposits. The research area records a typical example of this activity and illustrates that in addition to the strong Yanshanian tectonic magmatism and metallogenic activity that occurred on the northern margin of the North China Craton (Hua and Mao, 1999; Zhai, 2010), there was at least one other period of large-scale Indosinian alkaline magmatism and related Au and Mo mineralization, which led to the formation of the large-sized Hadamengou gold deposits that differ from the products of the Mesozoic metallogenic explosion in the North China Craton.

CONCLUSIONS

(1) The geochemical properties of the Dongshadegai pluton include high Si content, high alkali contents, and weakly peraluminous characteristics, indicating that it is an A-type granite. The REE patterns of the samples show right-tilted curves with weak negative Eu anomalies. In addition, the samples are depleted of Nb, Ta, P, Ti, and Sr but are enriched in K, La, Ce, and Hf.

(2) The weighted average U-Pb age of the zircons from the Dongshadegai pluton is 236.0±2.7 Ma (MSWD=1.6), which corresponds to the Middle Triassic period. Thus, the Dongshadegai pluton is the product of Indosinian regional tectonic magmatism. In addition, the age

data and Pb isotope ratios show that the Dongshadegai pluton and the regional Au metallogenic deposits share a common origin, implying that both are products of the same regional tectonic magmatism.

(3) In addition to the strong Yanshanian tectonic magmatism and metallogenic explosion that occurred on the northern margin of the North China Craton, at least one other period of Indosinian alkaline magmatism and related Au and Mo metallogenic processes occurred. Determining a method to recognize and identify the mineral deposits formed by these metallogenic processes is a key question that should be addressed by future investigations.

ACKNOWLEDGEMENTS

This study was supported by the Natural Science Foundation of Hebei Province (Grant No. D2020501002) and the Fundamental Research Funds for the Central Universities (N172303015, N130423003). We would like to thank Dr. Gilles Chazot and the anonymous reviewers for their constructive comments, which have helped us improve this paper.

REFERENCES

Ahmad M. and Walshe J.L., 1990. Wall-rock alteration at the Emperor gold-silver telluride deposit, Fiji. Australian Journal of Earth Science 37, 189-199.

Anderson T., 2002. Correction of common Pb in U-Pb analyses that do not report ^{204}Pb. Chemical Geology 192, 59-79.

Badarch G., Cunningham W.D., Windley B.F., 2002. A new terrane subdivision for Mongolia: Implications for the Phanerozoic crustal growth of central Asia. Journal of Asian Earth Science 20, 87-100.

Boynton W.V., 1984. Cosmochemistry of the rare earth elements: Meteorite studies. In: Henderson, P. (Ed.), Rare Earth Element Geochemistry. Elsevier, Amsterdam, 63-114.

Brown G.C., Thorpe R.S., Webb P.C., 1984. The geochemical characteristics of granitoids in contrasting arcs and comments on magma sources. London, Blackwell Scientific, 413-426.

Cai M.H., Zhang Z.G., Qu W.J., 2011. Geological characteristics and Re-Os dating of the Chaganhua molybdenum deposit in Urad Rear Banner, western Inner Mongolia. Acta Geoscientica Sinica 32, 64-68.

Chao Y.Y., Wang M.J., Li J.M., Zhang D., Li G.Q., 2012. The geochemical character of trace elements of the Dongping gold deposit in Hebei Province, China. Mineral Deposits 31, 727-728.

Chen J.M., Liu G., Li C.C., 1996. Geology of greenstone-type gold deposits in the Wula-Daqing Mts., Inner Mongolia. Beijing: China Geological Publishing House, 1-165.

Chen B., Jahn B.M., Wilde S., 2000. Two contrasting Paleozoic magmatic belts in northern Inner Mongolia, China: Petrogenesis and tectonic implications. Tectonophysics 328, 157-182.

Collins, W.J., Beams, S.D., White, A.J.R., Chappell, B.W., 1982. Nature and origin of A-type granites with particular reference to Southeastern Australia. Contributions to Mineralogy and Petrology 80, 189-200.

Creaser R.A., Price R.C., Wormald R.J., 1991. A-type granite revisited-assessment of a residual-source model. Geology 19, 163-166.

Eby G.N., 1992. Chemical subdivision of the A-type granitoids: Petrogenetic and tectonic implications. Geology 20, 641-644.

Frost C.D. and Frost B.R., 1997. Reduced repakivi-type granite: The tholeiite connection. Geology 25, 647-650.

Frost B.R., Arculus R.J., Barnes C.G., 2001. A geochemical classification of granitic rocks. Journal of Petrology 42, 2033-2048.

Gan S.F., Qiu Y.M., Yang H.Y., VanReenen D.D., 1994. The Hadamengou Mine: A typical gold deposit in the Archean granulite facies terrane of the North China Craton. International Geology Review 36, 850-866.

Gao P., Zheng Y.F., Zhao ZF., 2016. Experimental metls from crustal rocks: a lithochemical constraint on granite petrogenesis. Lithos 266-267, 133-157.

Gu F.H., Zhang Y.M., Liu R.P., Deng G., Sun X., 2015. Magma mixing and mingling of the Shadegai granite in Inner Mongolia: Evidence from petrography, mineral chemistry and geochronology. Acta Petrologica Sinica 31, 1374-1390.

Han B.F., Wang S.G., Hong D.W., 1993. Age of Guangtoushan alkali granite, Pingquan, Hebei Province, China. Scientia Geologica Sinica 28, 183-185.

Hart C.J.R., Goldfarb R.J., Qiu Y.M., Snee L., Miller L.D., Miller M.L., 2002. Gold deposits of the northern margin of the North China Craton: multiple late Paleozoic- Mesozoic mineralizing events. Mineralium Deposita 37, 326-351.

Honarmand M., Li X.H., Nabatian G., Neubauer F., 2017. In-situ zircon U-Pb age and Hf-O isotopic constraints on the origin of the Hasan-Robat A-type granite from Sanandaj-Sirjan zone, Iran: implications for reworking of Cadomian are igneous rocks. Miner Petrol 111, 659-675.

Hou W.R., Nie F.J., Du A.D., Li C., Jiang S.H., Bai D.M., Liu Y., 2010. Re-Os isotopic dating of molybdenite from the Xishadegai molybdenum deposit in Urad Front Banner of Inner Mongolia and its geological significance. Mineral Deposits 29, 1043-1053.

Hou W.R., 2011. Contrast study on the Hadamengou gold deposit and Jinchanggouliang gold deposit, Inner Mongolia. Beijing: Chinese Academy of Geological Sciences, 1-109.

Hou W.R., Nie F.J., Hu J.M., Liu Y.F., Xiao W., Liu Y., Zhang K., 2011. Geochronology and Geochemistry of Shadegai Granite in Wulashan area, Inner Mongolia, and Its Geological Significance. Journal of Jilin University (Earth Science Edition) 41, 1914-1927.

Hua R.M. and Mao J.W., 1999. A preliminary discussion on the Mesozoic metallogenic explosion in East China. Mineral Deposits 18, 300-307.

Jackson S.E., Pearson N.J., Belousova E.A., 2004. The

application of laser ablation inductively coupled plasma-mass spectrometry to in situ U-Pb zircon geochronology. Chemical Geology 211, 47-69.

Jensen E.P. and Barton M.D., 2000. Gold deposits related to alkaline magmatism (in Gold in 2000). Review of Economic Geology 13, 279-314.

Kelley K.D. and Ludington S., 2002. Cripple Creek and other alkaline-related gold deposits in the southern Rocky Mountains, USA: Influence of regional tectonics. Mineralium Deposita 37, 38-60.

Kerrich R. and Watson G.P., 1984. The Macassa mine Archean lode gold deposit, Kirkland Lake, Ontario; geology, patterns of alteration, and hydrothermal regimes. Economic Geology 79, 1104-1130.

King P.L., Chappell B.W., Allen C.M., White A.J.R., 2001. Are A-type granites the high-temperture felsic granites? Evidence from fractionated granites of the Wangrah Suite. Australian Journal of Earth Sciences 48, 501-514.

Lamb M.A. and Badarch G., 1997. Paleozoic sedimentary basins and volcanic-arc system of southern Mongolia: New stratigraphic and sedimentological constructions. International Geology Review 39, 542-576.

Li D.P., Chen Y.L., Chen L.M., 2009. Zircon LA-ICP-MS study and petrogenesis simulation of Dahuabei pluton in the Wulashan area, Inner Mongolia. Progress in Natural Science 19, 1727-1737.

Li C.M., Deng J.F., Chen L.H., Su S.G., Li H.M., Hu S.L., Liu X.M., 2010. Two periods of zircon from Dongping gold deposit in Zhangjiakou-Xuanhua area, northern margin of North China: Constraints on metallogenic chronology. Mineral Deposits 29, 265-275.

Li J.Y., 2006. Permian geodynamic setting of Northeast China and adjacent regions: Closure of the Paleo-Asian Ocean and subduction of the Paleo-Pacific Plate. Journal of Asian Earth Sciences 26, 207-224.

Liu J.M., Zhao Y., Sun Y.L., 2010. Recognition of the latest Permian to Early Triassic Cu-Mo mineralization on the northern margin of the North China block and its geological significance. Gondwana Research 17, 125-134.

Ludwig K.R., 2001. Users Manual for Isoplot/Ex (rev. 2.49): A Geochronological Toolkit for Microsoft Excel. Berkeley Geochronology Center (Special Publication No.1a, 55).

Luo Z.K., Guan K., Miao L.C., 2002. Dating of the dykes and altered sericite in Jiapigou gold ore belt, Jilin Province, and its gold formation age. Geoscience 16, 19-25.

Luo Z.K., Miao L.C., Guan K., 2003. SHRIMP U-Pb zircon dating of the Dushan granitic batholith and related granite-porphyry dyke, eastern Hebei Province, and their geological significance. Geochimica 32, 173-180.

Maniar P.D. and Piccoli P.M., 1989. Tectonic discrimination of granitoids. Geological Society of America Bulletin 101, 635-643.

Mao J.W. and Li Y.Q., 2001. Fluid inclusions of the Dongping gold telluride deposit in Hebei Province, China: Involvement of mantle fluid in metallogenesis. Mineral Deposits 20, 23-36.

Martin R.F., 2006. A-type granites of crustal origin ultimately result from open-system fenitization-type reactions in an extensional environment. Lithos 91, 125-136.

Miao L.C., Fan W.M., Zhai M.G., Qiu Y.M., McNaughton N.J., Groves D.I., 2003. Zircon SHRIMP U-Pb geochronology of the granitoid plutons from Jinchanggouliang- Erdaogou gold deposits field and its significance. Acta Petrologica Sinica 19, 71-80.

Miao L.C., Qiu Y.M., Guan K., McNaughton N., Qiu Y.S., Luo Z.K., Groves D.I., 2000. SHRIMP chronological study of the granitoids and mineralization in the Hadamengou gold deposit, Inner Mongolia. Mineral Deposits 19, 182-190.

Miao L.C., Qiu Y.M., Guan K., McNaughton N., Qiu,Y.S., Luo Z.K., Groves D.I., 2001. A Chronological Study of SHRIMP U-Pb of zircon from the Dahuabei Pluton in the Wulashan area, Inner Mongolia. Geological Review 47, 169-174.

Middlemost E.A., 1994. Naming materials in the magma/igneous rock system. Earth Science Reviews 37, 215-224.

Mingram B., Trumbull R.B., Littman S., Gerstenberger H., 2000. A petrogenetic study of anorogenic felsic magmatism in the Cretaceous Paresis ring complex, Namibia: Evidence for mixing of crust and mantle-derived components. Lithos 54, 1-22.

Mou B.L. and Yan G.H., 1992. Geochemistry of Triassic alkaline or subalkaline igneous complexes in Yan-Liao area and their significance. Acta Geologica Sinica 66, 108-122.

Moghadam H.S., Li X.H., Ling X.X., Stern R.J., Santos J.F., Meinhold G., Ghorbani G., Shahabi S., 2015. Petrogenesis and tectonic implications of Late Carboniferous A-type granites and gabbronorites in NW Iran: Geochronological and geochemical constraints. Lithos 212-215, 266-279.

Muller D. and Groves D.I., 1997. Potassic igneous rocks and associated gold-copper mineralization. New York: Springer, 1-157.

Mushkin A., Navon O., Halicz L., Hartmann G., Stein M., 2003. The petrogenesis of A-type magmas from the Amram Massif, southern Israel. Journal of Petrology 44, 815-832.

Nie F.J., Pei R.F., Wu L.S., Zhang H.T., Bjorlykke A., 1994. Study on lead and sulfur isotopes of the quartz-K-feldspar-type gold deposit in Wulashan, Inner Mongolia Autonomous Area, P.R. China. Mineral Deposits 13, 106-117.

Nie F.J. and Bjorlykke R.A., 1994. Lead and sulfur isotopic studies of the Wulashan quartz-K-feldspar and quartz vein gold deposit, southwest Inner Mongolia, People's Republic of China. Economic Geology 89, 1289-1305.

Nie F.J., Jiang S.H., Su X.X., Wang X.L., 2002. Geological features and origin of gold deposits occurring in the Baotou-Bayan Obo district, south-central Inner Mongolia, People's Republic of China. Ore Geology Review 20, 139-169.

Nie F.J., Jiang S.H., Liu Y., Hu P., 2005. Re-discussions on the time limitation of gold mineralization occurring within

the Hadamengou deposit, south-central Inner Mongolia Autonomous Region. Acta Petrologia Sinica 21, 1719-1728.

Nie F.J., Zhang K., Liu Y.F., Jiang S.H., Liu Y., Liu Y., 2011. Indosinian magmatism and molybdenum, gold mineralization along the Northern Margin of the North China Craton and adjacent area. Journal of Jilin University (Earth Science Edition) 41, 1651-1656.

Pearce J.A,1996. Sources and settings of granitic rocks. Episodes 19, 120-125.

Rickwood P.C., 1989. Boundary lines within petrologic diagrams which use oxides of major and minor elements. Lithos 22, 247-263.

Sillitoe R.H., 2002. Some metallogenic features of gold and copper deposits related to alkaline rocks and consequences for exploration. Mineralium Deposita 37, 4-13.

Skjerlie K.P. and Johnston A.D., 1992. Vapor-absent melting at 10 kbar of a biotite- and amphibole-bearing tonalitic geneiss: implication for the generation of A-type granite. Geology 20, 263-266.

Song Y., Wang R.J., Nie F.J., 2011. The discovery of the Indosinian metallogenesis in the Jinchangyu gold deposit and its geological significance. Acta Geoscientica Sinica 32, 125-128.

Sun S.S. and McDonough W., 1989. Chemical and isotopic systematics of oceanic basalts: Implications for mantle composition and processes. Geological Society, London, Special Publication 42, 313-345.

Wan B., Hegner E., Zhang L.C., 2009. Rb-Sr geochronology of chalcopyrite from the Chehugou porphyry Mo-Cu deposit (Northeast China) and geochemical constraints on the origin of hosting granites. Economic Geology 104, 351-363.

Windley B.F., Alexeiev D., Xiao W., Kroner A., Badarch G., 2007. Tectonic models for the accretion of the Central Asian orogenic belt. Journal of the Geological Society 164, 31-47.

Whalen J.B., Currie K.L., Chappell B.W., 1987. A-type granites: Geochemical characteristics, discrimination and petrogenesis. Contributions to Mineralogy and Petrology 95, 407-419.

Wu F.Y., Sun D.Y., Jahn B.M., Wilde S., 2004. A Jurassic garnet-bearing granitic pluton from NE China showing tetrad REE patterns. Journal of Asia Earth Science 23, 731-744.

Wu F.Y., Sun D.Y., Li H.M., Jahn B.M., Wilde S., 2002. A-type granites in northeastern China: Age and geochemical constraints on their petrogenesis. Chemical Geology 187, 143-173.

Wu F.Y., Zhao G.C., Sun D.Y., 2007. The Hulan Group: Its role in the evolution of the Central Asian Orogenic Belt of NE China. Journal of Asian Earth Sciences 30, 542-556.

Xiao W., Windley B.F., Hao J., 2003. Accretion leading to collision and the Permian Solonker suture, Inner Mongolia, China: Termination of the central Asian orogenic belt. Tectonics 22, 1069-1077.

Xiao W.J., Windley B.F., Huang B.C., 2009. End-Permian to mid-Triassic termination of the accretionary processes of the southern Altaids: Implications for the geodynamic evolution, Phanerozoic continental growth, and metallogeny of Central Asia. International Journal of Earth Sciences 98, 1189-1217.

Yang J.H., Wu F.Y., Chung S.L., Wilde S.A., Chu M.F., 2006. A hybrid origin for the Qianshan A-type granite, Northeast China: Geochemical and Sr-Nd-Hf isotopic evidence. Lithos 89, 89-106.

Zartman R.E. and Doe B.R., 1981. Plumbotectonics - the model. Tectonophysics 75, 135-162.

Zeng Q.D., Liu J.M., Zhang Z.L., 2009. Ore-forming time of the Jiguanshan porphyry molybdenum deposit, northern margin of the North China Craton and the Indosinian mineralization. Acta Petrologia Sinica 25, 393-398.

Zhai M.G., 2010. Tectonic evolution and metallogenesis of the North China Craton. Mineral Deposits 29, 24-36.

Zhan M.G., 1998. Trend and progress in the study of the classification and emplacement mechanism of granitoids. Regional Geology of China 17, 182-188.

Zhang H.T., So C.S., Yun S.T., 1999. Regional geological setting and metallogenesis of central Inner Mongolia, China: Guides for exploration of mesothermal gold deposits. Ore Geology Review 14, 129-146.

Zhang Y.M., Gu X.X., Dong S.Y., Cheng W.B., Huang Z.Q., Li F.L., Yang W.L., 2011. Zircon U-Pb and molybdenite Re-Os dating for the Xishadegai molybdenum deposit in Inner Mongolia and its geological significance. Journal of Mineral and Petrology 31, 33-41.

Zhang Y.M., 2012. Metallogenesis, ore-controlling factors and prospecting direction of the Liubagou-Hadamengou gold deposit, Inner Mongolia. Beijing: China University of Geosciences, 1-108.

Zhang Y.M., Gu X.X., Sun X., Zhao W., Xiang Z.L., Liu R.P., 2018. Genesis of the Xishadegai Mo deposit in Inner Mongolia, North China: Constraints from geology, geochronology, fluid inclusion, and isotopic compositions. Geological Journal 53, 3110-3128.

Zhao Q.Y., Li G., Liu Z.H., Xu Z.Y., Li C.F., Wang W.Q.. Wang X.A., 2009. Characteristics and origin of the Shadegai pluton in the Daqingshan area, Inner Mongolia. Journal of Jilin University (Earth Science Edition) 39, 1073-1079.

Zhao Y., Chen B., Zhang S.H., Liu J.M., Hu J.M., Liu J., Pei J.L., 2010. Pre-Yanshanian geological events in the northern margin of the North China Craton and its adjacent areas. Geology in China 37, 900-915.

Zhou L.D., Zhao Z.H., Zhou G.F., 1996. Isotopic chronology of some alkaline rock bodies in China. Geochimica 25, 164-171.